Geophysical Research Letters

RESEARCH LETTER
10.1029/2025GL118040

Mitigated Rapid Temperature Variability in the Northern Mid-High Latitudes Under Carbon Neutrality

Pinya Wang[1,2], Fengchun Ye[1,2], Yang Yang[1,2], Jianping Tang[3], and Hong Liao[1,2]

[1]State Key Laboratory of Climate System Prediction and Risk Management/Jiangsu Key Laboratory of Atmospheric Environment Monitoring and Pollution Control/Jiangsu Collaborative Innovation Center of Atmospheric Environment and Equipment Technology/Joint International Research Laboratory of Climate and Environment Change, Nanjing University of Information Science and Technology, Nanjing, China, [2]School of Environmental Science and Engineering, Nanjing University of Information Science and Technology, Nanjing, China, [3]School of Atmospheric Sciences, Nanjing University, Nanjing, China

Abstract Rapid temperature variability (RTV) is a key indicator of short-term climate variability. This study assesses future RTV changes under carbon neutrality using multi-model outputs from the Coupled Model Intercomparison Project Phase 6 under the Shared Socioeconomic Pathway 1-1.9 (SSP1-1.9) scenario. We further perform attribution experiments with the fully coupled Community Earth System Model to quantify the role of greenhouse gases (GHGs), aerosols (AER), and tropospheric ozone (O_3) in driving projected RTV changes. Our results reveal a substantial decline in RTV across the Northern Hemisphere (NH) under carbon neutrality, especially at mid-to-high latitudes in winter and summer. This decline in RTV is primarily attributed to reduced temperature advection variability and changes in daily net surface radiative forcing. Reductions in aerosols exert the strongest impacts on RTV, surpassing the effects of GHGs and tropospheric O_3. The findings highlight the critical role of aerosol reductions in modulating short-term climate fluctuation.

Plain Language Summary Rapid fluctuations between daily temperature are projected to decline across much of the Northern Hemisphere by mid-century under the carbon neutrality pathway. The multi-model analysis shows that this dampening is driven mainly by weaker temperature advection and smaller day-to-day changes in how much solar and terrestrial radiation reaches the surface. Among different climate drivers that we focus on, that is, greenhouse gases, aerosols, and tropospheric ozone, reductions in aerosols and their precursors exert the largest effects on reducing the rapid temperature variability. This means that cleaning up air pollution will play a key role in shaping the short-term temperature variability under a carbon neutrality future.

Key Points:

- Carbon neutrality leads to a widespread reduction in Rapid temperature variability (RTV) in the Northern Hemisphere by the mid-century
- Projected decreases in RTV are jointly driven by weakened Temperature Advection and DTDNRF
- Among greenhouse gases, aerosols, and tropospheric ozone, aerosol reductions play the dominant role in RTV response under carbon neutrality

Supporting Information:

Supporting Information may be found in the online version of this article.

Correspondence to:

Y. Yang,
yang.yang@nuist.edu.cn

Citation:

Wang, P., Ye, F., Yang, Y., Tang, J., & Liao, H. (2025). Mitigated rapid temperature variability in the northern mid-high latitudes under carbon neutrality. *Geophysical Research Letters*, *52*, e2025GL118040. https://doi.org/10.1029/2025GL118040

Received 11 JUL 2025
Accepted 13 OCT 2025

1. Introduction

Human activities emit a variety of substances that influence the Earth's climate system, among which greenhouse gases (GHGs), aerosols, and tropospheric ozone are the primary drivers, yet playing distinct roles. GHGs, such as carbon dioxide (CO_2), methane (CH_4), and nitrous oxide (N_2O), trap longwave radiation in the atmosphere and contribute to long-term global warming. Their accumulation leads to a positive radiative forcing, driving increases in both mean temperatures and the frequency of extreme heat events (Irfan et al., 2024; Van Wijngaarden et al., 2020). Aerosols, on the other hand, affect climate change by altering the Earth's energy budget, primarily through scattering and/or absorbing solar radiation (Ren et al., 2024; N. Yang et al., 2024). For instance, sulfate and nitrate aerosols scatter incoming solar radiation, producing a localized cooling effect (Xu & Penner, 2012), while black carbon absorbs solar radiation, warms the atmosphere, and accelerates ice and snow melting (B. Zhang, 2020). Tropospheric ozone, though not directly emitted, is a secondary pollutant formed by photochemical reactions involving precursor gases such as Nitrogen Oxides (NO_x) and Volatile Organic Compounds. It acts as a short-lived climate forcer with a positive radiative forcing effect (Boynard et al., 2025; Yao et al., 2025). Rising tropospheric ozone concentrations not only contribute to surface warming but also pose threats to human health and vegetation (Ebi & McGregor, 2008; Fuhrer et al., 2016).

In response to the escalating climate risks, the 21st Conference of the Parties to the United Nations Framework Convention on Climate Change (COP21) adopted the Paris Agreement, a landmark international climate treaty. The agreement sets a long-term goal of limiting the increase in global average temperature to well below 2°C above pre-industrial levels, while pursuing efforts to restrict the rise to 1.5°C (Schleussner et al., 2016). The carbon neutrality pathway is expected to substantially mitigate global warming and realize the goals of the Paris

Agreement (Fankhauser et al., 2022; Huang & Zhai, 2021). Carbon neutrality is projected to not only reduce global mean temperature but also alleviate the occurrence of extreme weather events (Lei et al., 2022; F. Wang et al., 2021; J. Zhang & You, 2023). Moreover, the substantial reduction of anthropogenic emissions under carbon neutrality would also benefit air quality in the future (P. Wang et al., 2023; Y. Yang et al., 2024).

While the projected long-term trends in mean and extreme temperatures have been extensively investigated (e.g., Fischer & Schär, 2009; F. Guo et al., 2021; P. Wang et al., 2023), rapid temperature variability (RTV) provides new insights into short-term climate variability and its direct societal relevance, thereby offering a distinct and policy-relevant perspective that complements existing studies. For instance, the day-to-day fluctuations in air temperatures have direct implications for ecosystems, human health, and socioeconomic activities (Ge et al., 2022; Katz & Brown, 1992; Schär et al., 2004). Studies show that increases in RTV often leads to a rise in associated extreme weather events (Katz & Brown, 1992; Schär et al., 2004), elevated mortality risks associated with chronic and epidemic diseases (Y. Guo et al., 2011; Q. Liu et al., 2020; Zhan et al., 2017), reduced crop yields (Wheeler et al., 2000). Particularly, increased RTV could suppress economic growth, especially in low-latitude, low-income regions (Kotz et al., 2021), thereby worsening the existing unequal burden of climate change impacts across regions and socioeconomic groups. Therefore, insights into future RTV changes are essential for guiding climate adaptation and mitigation strategies.

In this study, we assess the future projected RTV by the mid-century with multi-model simulations under the Shared Socioeconomic Pathway 1-1.9 (SSP1-1.9) scenario from the Coupled Model Intercomparison Project Phase 6 (CMIP6). SSP1-1.9 represents a stringent mitigation pathway consistent with global carbon neutrality goals, and it is widely used to evaluate climate impacts under carbon neutrality (Kamal et al., 2021; P. Wang et al., 2023; Zhu et al., 2023). To further clarify the potential mechanisms underlying RTV change, we incorporate diagnostics based on the thermodynamic energy equation, clarifying the roles of atmospheric dynamics and radiative processes. In addition, we conduct an attribution analysis of projected RTV changes under carbon neutrality using the fully coupled Community Earth System Model (CESM), focusing on the individual and combined effects of anthropogenic GHGs, aerosols, and tropospheric ozone emissions following the SSP1-1.9 scenario. The remainder of this paper is organized as follows. Section 2 describes the model configuration, experimental design, and diagnostic methods. Section 3 presents the spatial and temporal characteristics of RTV under the carbon neutrality scenario. Section 4 explores the physical mechanisms driving RTV changes based on the thermodynamic energy budget analysis and provides the attribution results, highlighting the contributions of GHGs, aerosols, and tropospheric ozone. Finally, Section 5 summarizes the key findings and offers concluding remarks.

2. Data and Methods

2.1. Model Description

In this study, we employ fully coupled CESM version 1 (CESM1) to investigate the impacts of changes in anthropogenic GHGs, aerosols, and tropospheric ozone on temperature variability under the carbon neutrality pathway. CESM1 is a comprehensive Earth system model that integrates multiple components, including the Community Atmosphere Model (CAM) for atmospheric processes, the Parallel Ocean Program (POP) for ocean dynamics, the Community Land Model for terrestrial processes, and the Community Ice CodE (CICE) for sea ice simulation (J. Gao et al., 2023; Hurrell et al., 2013). These component models can be coupled in various configurations to simulate interactions among the carbon-nitrogen cycle, human-induced vegetation changes, land use dynamics, and the direct and indirect effects of aerosols on the climate system (He et al., 2015). In this work, the atmospheric component uses CAM version 5 (CAM5), configured at a horizontal resolution of $1.9° \times 2.5°$ with 30 vertical levels. The ocean component is based on POP version 2 (POP2) (P. Wang et al., 2023). Aerosol processes are represented using the three-mode version of the Modal Aerosol Module (MAM3) in CAM5, which includes major aerosol species such as black carbon, primary organic matter, secondary organic aerosols, sulfate, mineral dust, and sea salt, distributed across four log-normal size modes: Aitken, accumulation, coarse, and primary carbon modes (X. Liu et al., 2016). Additionally, following H. Wang et al. (2013), we incorporate model modifications to enhance aerosol convective transport and wet deposition processes.

2.2. Experimental Design

Following P. Wang et al. (2023), we use four sets of CESM1 simulations to examine the impacts of anthropogenic GHGs, aerosols, and tropospheric ozone (O_3) emissions on temperature variability under a carbon neutrality pathway. Specifically, major GHGs include carbon dioxide (CO_2), methane (CH_4), nitrous oxide (N_2O), and halocompounds (CFC-11 and CFC-12). The global mean concentrations of the major GHGs for 2020 and 2050 are listed in Table S1 in Supporting Information S1. Note that, in pace with the strict control of anthropogenic emissions under carbon neutrality, GHG show slight increases in the global mean CO_2, while anthropogenic aerosols and their precursors, and tropospheric ozone levels exhibit obvious decreases significantly by the mid of the century (Figures S1 and S2 in Supporting Information S1). These experiments are referred to as Baseline, GHG2050, AerGHG2050, and ALL2050. In all experiments, the projected GHG concentrations, emissions of aerosols and their precursors as well as tropospheric ozone concentrations, follow the SSP1-1.9 scenario. In Baseline, GHGs, aerosols and tropospheric ozone levels are all fixed at their 2020 levels. In GHG2050, GHG emissions are set to 2050 levels, while aerosols and ozone remain at 2020 levels. In AerGHG2050, both GHGs and aerosols are fixed at 2050 levels, while tropospheric ozone remains at 2020 levels. In the ALL2050 experiment, the GHGs, aerosols, and tropospheric ozone levels are all fixed at 2050. All experiments have three ensemble members with a small initial perturbation and run for at least 200 years, of which the last 100 years are used for analyses. Thus, the impacts of different components on temperature variability under carbon neutrality are evaluated through a series of pairwise comparisons: GHG2050 versus Baseline isolates the effect of future GHG changes; AerGHG2050 versus GHG2050 quantifies the specific contribution of aerosol reductions; and ALL2050 versus AerGHG2050 assesses the impact of tropospheric ozone changes.

2.3. CMIP6 Multi-Model Simulations

We utilize daily near surface air temperatures, 10-m winds, shortwave and longwave radiation of multi-model simulations (see Table S2 in Supporting Information S1 for details) from CMIP6 to project the future changes in RTV changes and assess the possible mechanisms. We focus on two representative time periods the current period of 2020s (average for 2015–2024) and 2050s (average for 2045–2054). The multi-model ensemble mean (MME) is applied for all analyses.

2.4. ERA5 Reanalysis

For model validations, we adopted T2m obtained from the European Centre for Medium-Range Weather Forecasts (ECMWF) reanalysis Version 5 (ERA5) for the period 2015–2024. The ERA5 data set provides hourly estimates of a wide range of atmospheric, land, and oceanic variables globally, from January 1940 to the present (Soci et al., 2024). Both ERA5 reanalysis and CMIP6 multi-model simulations are regridded to a uniform spatial resolution of 1.9° × 2.5° as that of CESM1 to ensure consistency across models.

2.5. Definition of Rapid Temperature Variability

In this study, we adopt the widely used metric of day-to-day temperature variability (DTDT) to characterize the future changes of RTV (Bonacci et al., 2022; Ge et al., 2022; Tang et al., 2021). It refers to the average absolute difference in T2m between two consecutive days within the study period, which is obtained equation as follows:

$$\mathrm{DTDT} = \frac{1}{n-1}\sum_{i=1}^{n-1}|T_{i+1} - T_i| \tag{1}$$

where T_i represents T2m on day i and n represents the total number of days in the study period.

2.6. Diagnostic Decomposition of DTDT Based on Thermodynamic Energy Equation

According to thermodynamic energy equation (Wallace & Hobbs, 2006), the mean temperature difference between two adjacent days can be expressed as:

$$\delta T = \frac{\partial T}{\partial t} = -v \cdot \nabla T + \left(\frac{RT}{c_p P} - \frac{\partial T}{\partial P}\right)\omega + \frac{1}{c_p}\frac{\partial Q}{\partial t} \tag{2}$$

where T represents the near-surface daily mean T2m (°C), v denotes the daily mean 10-m vector wind (m s^{-1}), ∇ represents the horizontal divergence operator, ω is the near-surface daily mean vertical velocity (Pa s^{-1}), P is the atmospheric pressure (Pa), and Q is the daily mean diabatic heating. In the equation, R represents the specific gas constant for dry air (287 J K^{-1} kg^{-1}), and c_p is the specific heat capacity of dry air at constant pressure (1,004 J K^{-1} kg^{-1}).

Following Ge et al. (2022), combining Equation 2 and Equation 1, DTDT can be expressed as follows:

$$\mathrm{DTDT} = \frac{1}{n-1}\sum_{i=1}^{n-1}|\delta T_i| = \frac{1}{n-1}\sum_{i=1}^{n-1}\left|\frac{\partial T}{\partial t_i}\right| \tag{3}$$

Substituting Equation 2, DTDT can be expressed as the sum of the following three terms to diagnose the relative contribution of each term:

$$\mathrm{term1} = \frac{1}{n-1}\sum_{i=1}^{n-1}|-v\cdot\nabla T| \tag{4}$$

$$\mathrm{term2} = \frac{1}{n-1}\sum_{i=1}^{n-1}\left|\left(\frac{RT_i}{c_pP_i} - \frac{\partial T}{\partial P_i}\right)\omega_i\right| \tag{5}$$

$$\mathrm{term3} = \frac{1}{n-1}\sum_{i=1}^{n-1}\left|\frac{1}{c_p}\frac{\partial Q}{\partial t}_i\right| \tag{6}$$

Therefore, future changes in DTDT (ΔDTDT) by mid of the century can be expressed as:

$$\Delta\mathrm{DTDT} = \Delta\mathrm{term1} + \Delta\mathrm{term2} + \Delta\mathrm{term3} \tag{7}$$

where Δ represents the difference between the periods of 2050s and 2020s. Δterm1 indicates the changes in daily mean near-surface horizontal temperature advection (ΔTADV), Δterm2 represents changes in daily mean adiabatic compression and vertical advection, with negligible magnitude and can typically be neglected (Q. Liu, 2021), and Δterm3 denotes changes in daily mean diabatic heating rate.

Furthermore, Δterm1 can be derived into the zonal and meridional parts and assess their relative contribution, as follows:

$$\Delta\mathrm{term1} = \Delta\left(\frac{1}{n-1}\sum_{i=1}^{n-1}|-V\cdot\nabla T|\right) = \Delta\left(\frac{1}{n-1}\sum_{i=1}^{n-1}\left|-u\cdot\frac{\partial T}{\partial x}\right|\right) + \Delta\left(\frac{1}{n-1}\sum_{i=1}^{n-1}\left|-v\cdot\frac{\partial T}{\partial y}\right|\right) \tag{8}$$

In this work, Δterms3 specifically considers changes in the surface net radiation forcing (NRF), that is, the sum of net surface shortwave and longwave radiative forcing, as changes in GHGs, aerosols and tropospheric ozone primarily modulate solar and longwave radiative forcing (Z. Gao et al., 2009; Kim et al., 2017). Δterm3 can be expressed as:

$$\Delta\mathrm{term3} = \Delta\left(\frac{1}{n-1}\sum_{i=1}^{n-1}\left|\frac{\partial\mathrm{NRF}}{\partial t_i}\right|\right) = \Delta\left(\frac{1}{n-1}\sum_{i=1}^{n-1}|\mathrm{NRF}_{i+1} - \mathrm{NRF}_i|\right) \tag{9}$$

Here, NRF_i represents the surface net radiation forcing on day i and Δterm3 is characterize the changes in the daily-to-day variability of NRF (DTDNRF). Note that the unit of Δterm3 is W/m^2, not same as DTDT, thus it can provide a qualitative interpretation of the projected change in DTDT.

3. Projected Changes in DTDT by the Mid-Century Under Carbon Neutrality

Model evaluations demonstrate that both CESM1 and the CMIP6 MME can reproduce the spatial distribution and magnitude of mean surface air temperature and DTDT over the Northern Hemisphere (NH) during the 2020s (see Text S1, Figures S3 and S4 in Supporting Information S1). Subsequently, we examine the projected changes in

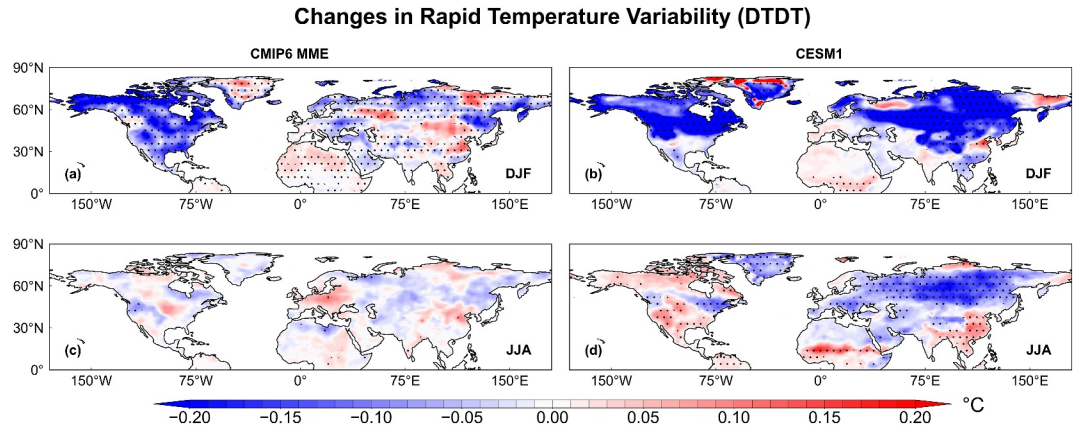

Figure 1. Spatial distributions of projected changes in DTDT in 2050s relative to 2020s with Coupled Model Intercomparison Project Phase 6 multi-model ensemble mean under (a, c) SSP1-1.9 scenario and (b, d) CESM1 simulations. The upper and lower panels show the changes in wintertime (DJF) and summertime (JJA), respectively. The dotted areas pass the 95% confidence level of a two-tailed *t*-test.

DTDT by mid of the century relative to the current climate, based on both CESM1 and CMIP6 MME results (see Figure 1). Note that the projected changes in DTDT based on CMIP6 simulations are estimated as the difference between 2050s and 2020s, whereas in CESM1, changes are derived from the difference between the ALL2050 and the Baseline experiments.

For winter, CMIP6 MME projects a widespread decrease in DTDT across NH, particularly over North America and mid-high latitudes of Eurasia, with maximum reductions exceeding −0.2°C, while increases in DTDT are seen over Greenland, North Africa, and East Asia regions (Figure 1a). CESM1 simulation exhibits a broadly similar wintertime pattern, with widespread DTDT reductions across NH, especially over North America and Eurasia, although they show smoother spatial features and more localized increases over regions such as Greenland and tropical Africa (Figure 1b). The projected changes of summertime DTDT based on CESM1 and CMIP6 MME show similar spatial patterns with those of wintertime DTDT. Specifically, CMIP6 MME shows modest decreases of DTDT over most of North America and Eurasia while slight increases in DTDT are found over regions including North Africa, western Europe, and parts of East Asia. The CESM1 simulations also show regionally varied changes, with notable DTDT reductions over the mid-high latitudes of northern Eurasia but increases over North America, tropical Africa, and East Asia. Despite these regional differences, both CMIP6 and CESM1 suggest a less pronounced decline in DTDT during summer compared to winter, highlighting the seasonal contrast in RTV responses under carbon neutrality. To further assess the robustness of our results, we conducted a sign consistency test for the projected changes in DTDT based on the CMIP6 MME. The results show that, across most regions of the NH, the projected DTDT changes pass the consistency test that more than four out of six individual models exhibiting the same sign of change as the MME projection (Figure S5 in Supporting Information S1).

4. Possible Mechanisms Underlying Projected Changes in DTDT

In this section, we conduct a qualitative analysis to elucidate the potential mechanisms of projected changes in DTDT based on the thermodynamic energy equation under carbon neutrality. According to the thermodynamic energy equation (see Section 2.6), the projected changes in DTDT can primarily be attributed to changes in near-surface horizontal TADV (ΔTADV) and net near-surface radiative forcing (DTDNRF).

4.1. Projected Changes in Horizontal Temperature Advection

Figure 2 illustrates the spatial pattern of ΔTADV for 2050s relative to the 2020s under carbon neutrality, based on both CMIP6 and CESM1 simulations. ΔTADV represent an important dynamical factor influencing DTDT by modulating the transport and dispersion of thermal anomalies. In winter (DJF), both CMIP6 MME (Figure 2a) and CESM1 (Figure 2b) show widespread negative ΔTADV over high-latitude regions of North America and Eurasia, indicating a reduced contribution of warm or cold air advection, which in turn contributes to the decline in DTDT

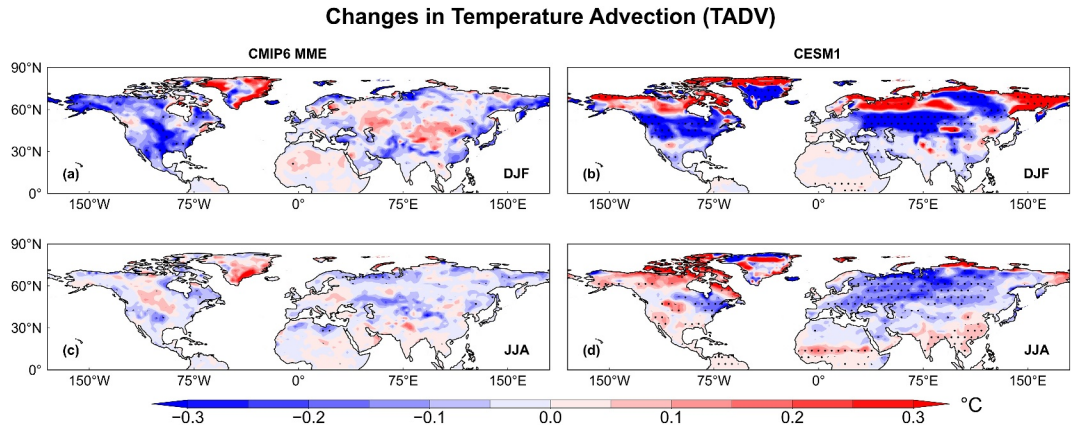

Figure 2. Spatial distributions of projected changes in Temperature Advection in 2050s relative to 2020s with Coupled Model Intercomparison Project Phase 6 multi-model ensemble mean under (a, c) SSP1-1.9 and (b, d) CESM1 simulations. The upper and lower panels show the changes in wintertime (DJF) and summertime (JJA), respectively. The dotted areas pass the 95% confidence level of a two-tailed *t*-test.

in these regions, consistent with the pronounced decrease in DTDT in Figure 1. The weakened TADV may result from a more stable atmospheric state or weaker synoptic activity, reducing day-to-day temperature fluctuations (Piskala & Huth, 2020). Conversely, positive ΔTADV is projected over Greenland and northeastern Eurasia, especially in the CESM1 simulation, suggesting an enhanced advection effect that contributes to local increases in DTDT (Figure 2b). In summer, the spatial patterns of ΔTADV changes are weaker and more heterogeneous. The CMIP6 MME shows small positive anomalies in regions such as southern Europe, North Africa, and East Asia (Figure 2c), which correspond to the areas of slight DTDT increase (Figure 1). The CESM1 simulation also indicates localized increases in ΔTADV over northern Africa and mid-latitude Eurasia (Figure 2d), which may explain the moderate increases in DTDT over these regions. However, in most parts of northern Eurasia, ΔTADV becomes more negative, potentially contributing to the strong decline in DTDT. Overall, the reduction in TADV under carbon neutrality, particularly in winter and over high latitudes, plays a crucial role in suppressing DTDT. These dynamical changes are more pronounced in CESM1 due to its smoother representation of atmospheric circulation, whereas CMIP6 results show greater spatial variability across models (not shown).

We further decomposed ΔTADV into its meridional and zonal components. The spatial distributions of meridional and zonal decompositions of ΔTADV for both CMIP6 MME and CESM1 simulations are shown in Figures S6–S9 in Supporting Information S1. In CMIP6 simulations, the projected changes in meridional and zonal TADV during winter exhibit similar patterns and comparable magnitudes, with decreases over North America, Southern and Eastern Asia, and increases over western and central Eurasia (Figures S6a and S7a in Supporting Information S1). In summer, both the meridional and zonal TADV components show broadly similar spatial patterns and magnitude, yet demonstrating higher spatial variability and weaker magnitudes compared to wintertime (Figures S6d and S7d in Supporting Information S1). Note that the projected changes in meridional and zonal components of TADV in either winter or summer are associated with substantial changes in both surface air temperature gradient (Figures S6b, S7b, S6e, and S7e in Supporting Information S1) and wind components (Figures S6c, S7c, S6f, and S7f in Supporting Information S1). And components of two different directions show similar spatial patterns and comparable magnitudes but with stronger changes in winter than summer, supporting the intensified changes in TADV and DTDT in winter and summer.

Similar results are found in the CESM simulations (Figures S8 and S9 in Supporting Information S1), supporting the hypothesis that future projected changes in horizontal TADV are attributed to variations in both meridional and zonal temperature components. And these variations are jointly driven by changes in the corresponding temperature gradients and wind components.

4.2. Projected Changes in Day-to-Day Variability of Near-Surface Radiative Forcing

In addition to dynamical processes, projected changes in diabatic heating, particularly the changes in daily variability of net near-surface radiative forcing (ΔDTDNRF), is a crucial thermodynamic driver of ΔDTDT. NRF

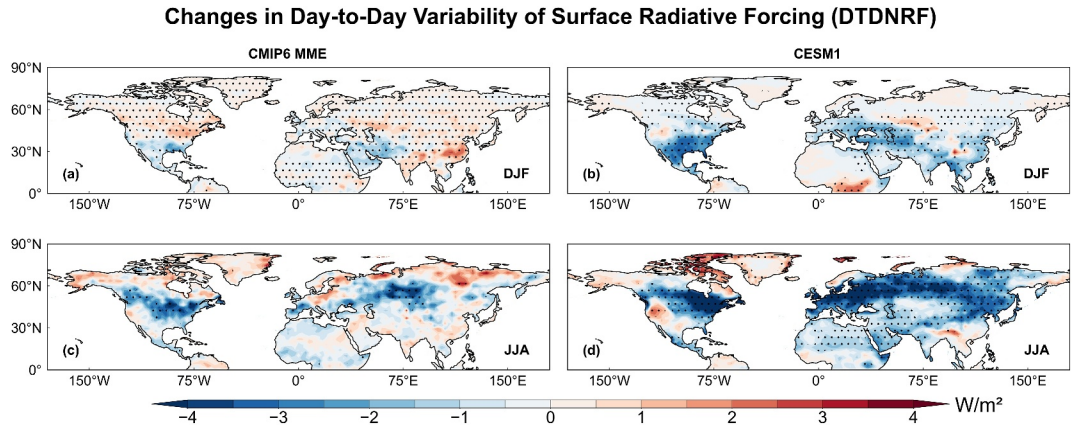

Figure 3. Spatial distributions of projected changes in day-to-day variability of surface net radiative forcing (DTDNRF) in 2050s relative to 2020s from Coupled Model Intercomparison Project Phase 6 multi-model ensemble mean under (a, c) SSP1-1.9 and (b, d) CESM1 simulations. The upper and lower panels show the changes in wintertime (DJF) and summertime (JJA), respectively. The dotted areas pass the 95% confidence level of a two-tailed *t*-test.

combine net shortwave and longwave radiation at the surface, which is sensitive to shifts in GHGs and aerosols. Figure 3 illustrates the projected changes in DTDNRF for the 2050s relative to the 2020s, based on both CMIP6 MME and CESM1 simulations. During winter, the CMIP6 MME shows slight positive DTDNRF anomalies over large portions of the NH mid-to-high latitudes, especially northern Eurasia and North America (Figure 3a). In summer, the DTDNRF changes in CMIP6 MME (Figure 3c) exhibit high magnitude and more regional variability. Negative DTDNRF anomalies dominate over parts of eastern Europe, East Asia, and North America, reinforcing the DTDT suppression during the warm season. However, localized positive anomalies in southern Europe and the Sahel may contribute to weak DTDT increases (Figure 1c). As highlighted above, in contract to the higher magnitude of DTDNRF changes in summer, DTDT changes are more pronounced in winter, suggesting DTDNRF may play a secondary role than DTDNRF in modulating DTDT changes.

The projected changes in DTDNRF with CESM1 simulations reveal a more spatially coherent and smoother pattern. In winter (Figure 3b), DTDNRF exhibit substantial reductions across most of North America, northern Eurasia, and Greenland, consistent with the strong DTDT declines (Figure 1b). In summer (Figure 3d), negative DTDNRF anomalies expand across nearly the entire NH, particularly over Eurasia, where they coincide with the suppressed DTDT seen in CESM projections (Figure 1d). Notably, consistent with CMIP6 MME, CESM1 projects a more widespread radiative damping effect on short-term temperature variability in summer than winter, reversing the higher magnitude of DTDT changes in winter, supporting the more prominent role of TADV changes.

In summary, both CMIP6 and CESM1 simulations indicate that the projected decreases in DTDT across most mid-to-high latitudes under carbon neutrality are jointly driven by changes in horizontal TADV and daily variability of radiative forcing. And horizontal TADV playing a more important role in shaping future short-term temperature variability.

4.3. Attribution of DTDT Changes to GHG, Aerosol, and Tropospheric Ozone Under Carbon Neutrality

With the fully coupled CESM1 simulations, we further quantify the individual contributions of the key anthropogenic climate drivers, that is, GHGs, aerosols, and tropospheric ozone, to projected changes DTDT under the carbon neutrality pathway (Figure 4). In winter, the GHG concentration changes lead to a notable DTDT reduction (>0.2°C) over central North America and northern Eurasia (Figure 4a), likely due to enhanced radiative forcing and associated atmospheric stabilization (Hansen et al., 1997; Irfan et al., 2024). In contrast, summer DTDT under GHG forcing increases slightly across most of North America, while remaining relatively unchanged in Eurasia (within ±0.1°C, Figure 4d), indicating seasonal asymmetry of DTDT changes to the GHG response. The impact of aerosol reductions is more spatially extensive and dominant. In both seasons, DTDT decreases significantly across NH, particularly in high-latitude regions (Figures 4b and 4e). The magnitude of reduction exceeds 0.5°C in winter and 0.15°C in summer. This widespread suppression of DTDT may be driven

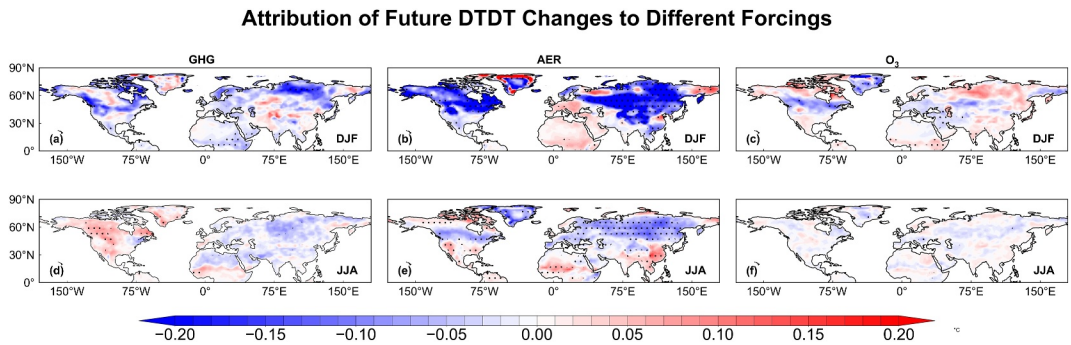

Figure 4. Spatial distributions of changes in DTDT in 2050s relative to 2020s under (a, d) greenhouse gas, (b, e) AER, and (c, f) O_3 from CESM1 simulations. The upper and lower panels show the changes under different forcings in wintertime (DJF) and summertime (JJA), respectively. The dotted areas pass the 95% confidence level of a two-tailed *t*-test.

by the weakening of the meridional temperature gradient in NH midlatitudes associated with reduced aerosol levels (Fahrenbach & Bollasina, 2023; Westervelt et al., 2015; Xiang et al., 2023). The effects tropospheric ozone changes are more localized and weaker. In winter, DTDT slightly increases at high latitudes of Eurasia but decreases over North America and central Eurasia (Figure 4c). In summer, DTDT declines modestly over most land regions (Figure 4f). In summary, aerosol reductions dominate the projected DTDT changes under carbon neutrality, exerting a stronger and more widespread dampening effect than GHGs or tropospheric ozone. Note that different climate forcers affect DTDT through their effects on both TADV and DTDNRF (not shown). P. Wang et al. (2023) indicated that aerosol changes would dominate the future changes in climate and extreme weather events by mid-century under carbon neutrality. Aerosols, as short-lived climate forcers, exhibit strong day-to-day variability that alters surface radiation and near-surface temperature (Y. Gao et al., 2022; Li et al., 2017), which thereby could modulate RTV. Our results highlight the critical role of aerosols in modulating short-term temperature variability and suggest that aerosol-climate interactions will play a central role in shaping synoptic and sub-seasonal climate variability in a carbon neutral future.

5. Conclusions and Discussion

Based on multi-model simulations from CMIP6, we reveal a robust decline in DTDT in both summer and winter seasons across NH under a carbon neutrality scenario by the mid-21st century. The decrease is particularly pronounced in winter and over mid to high latitude regions of Eurasia and North America. In contrast, summer DTDT exhibits more spatial heterogeneity but still tends toward a net reduction. Particularly, the projected reduction in DTDT over northern mid-to-high latitudes under carbon neutrality is jointly driven by weakened horizontal TADV and decreased daily variability of surface net radiative forcing, of which the reduced TADV plays a more important role, especially at high latitudes. And both meridional and zonal temperature gradients and wind components contribute to the advection changes.

Through a series of CESM1 simulations that isolate the effects of major anthropogenic climate drivers, GHGs, aerosols, and tropospheric ozone, and we find that aerosol emission reductions are the dominant driver of projected DTDT changes. Compared to the more modest influence of GHG increases and ozone reductions, aerosol reductions alone contribute to more than 0.5°C decreases in DTDT over large portions of the NH, especially during boreal winter. The pronounced seasonality of DTDT changes likely arises from different driving mechanisms in each season. In winter, DTDT is primarily controlled by strong warm-cold air mass advection while it is governed more by local diabatic processes in summer (Adams et al., 2021; Hamal & Pfahl, 2024; Horton et al., 2015). The stronger DTDT changes in winter than summer reflect the higher sensitivity of large-scale dynamical processes in winter compared with the response of local diabatic processes in summer under climate change. The findings are consistent with previous studies that a decrease in aerosols leads to a reduction in the meridional temperature gradient and winds over NH (An et al., 2023; Dong et al., 2022).

These findings suggest that aerosol reductions are crucial for improving air quality, they can also lead to a dampening of short-term temperature variability, which may indicate decreased weather extremes. Wu et al. (2025) suggest project an enhanced cold-warm flip extremes in the future under high emission scenario

SSP5-8.5 relative to the low emission scenarios, which may be likely driven by the reduced DTDT. Thus, projected changes in RTV and the associated mechanisms deserve further attention. However, model-specific sensitivities, such as the strong aerosol response in CESM1, may also introduce uncertainties (Fan et al., 2018; Zeng et al., 2021). While overall warming favors more frequent high-temperature extremes such as heatwaves by the mid of the century (e.g., P. Wang et al., 2023), the lower RTV implies fewer abrupt cold-to-warm transitions. Furthermore, the reduced RTV suggests that extreme events may persist for a prolonged duration once they occur, a phenomenon that warrants further research attention.

This study has both academic and policy relevance. Academically, it advances understanding of short-term temperature variability under future climate scenarios, an aspect less examined than mean temperature, and clarifies the roles of GHGs, aerosols, and ozone. From a policy perspective, our findings highlight that mitigation strategies should simultaneously consider environmental benefits, such as air quality improvement, and climate impacts. Note that this study assesses the dominant effects of individual climate forcers but does not account for their interactions. For instance, aerosols can influence O_3 chemistry through heterogeneous and multiphase reactions (Liao et al., 2004). The climate impacts of such interactions warrant further investigation.

Conflict of Interest

The authors declare no conflicts of interest relevant to this study.

Data Availability Statement

The CMIP6 model result can be found at https://esgf-node.llnl.gov/projects/cmip6. ERA5 reanalysis data are provided by the Copernicus Climate Change Service (C3S) (Hersbach et al., 2023). The processed modeling data are available at P. Wang (2025).

Acknowledgments
This study was supported by the National Key Research and Development Program of China (Grant 2024YFF0811400), the National Natural Science Foundation of China (Grants 42521006 and 42475032), and the Natural Science Foundation of Jiangsu Province (Grant BK20241902).

References

Adams, R. E., Lee, C. C., Smith, E. T., & Sheridan, S. C. (2021). The relationship between atmospheric circulation patterns and extreme temperature events in North America. https://doi.org/10.1002/joc.6610

An, X., Chen, W., Li, C., Sheng, L., Zhang, W., Hai, S., & Hu, P. (2023). Influence of rainfall-induced diabatic heating on southern rainfall-northern haze over eastern China in early February 2023. *Science China Earth Sciences*, *66*(11), 2579–2593. https://doi.org/10.1007/s11430-023-1181-3

Bonacci, O., Roje-Bonacci, T., & Vrsalović, A. (2022). The day-to-day temperature variability method as a tool for urban heat island analysis: A case of Zagreb-Grič Observatory (1887–2018). *Urban Climate*, *45*, 101281. https://doi.org/10.1016/j.uclim.2022.101281

Boynard, A., Wespes, C., Hadji-Lazaro, J., Sinnathamby, S., Hurtmans, D., Coheur, P. F., et al. (2025). Tropospheric ozone assessment report (TOAR): 16-year ozone trends from the IASI climate data record. *Atmospheric Chemistry and Physics*. https://doi.org/10.5194/egusphere-2025-1054

Dong, B., Sutton, R. T., Shaffrey, L., & Harvey, B. (2022). Recent decadal weakening of the summer Eurasian westerly jet attributable to anthropogenic aerosol emissions. *Nature Communications*, *13*(1), 1148. https://doi.org/10.1038/s41467-022-28816-5

Ebi, K. L., & McGregor, G. (2008). Climate change, tropospheric ozone and particulate matter, and health impacts. *Environmental Health Perspectives*, *116*(11), 1449–1455. https://doi.org/10.1289/ehp.11463

Fahrenbach, N. L., & Bollasina, M. A. (2023). Hemispheric-wide climate response to regional COVID-19-related aerosol emission reductions: The prominent role of atmospheric circulation adjustments. *Atmospheric Chemistry and Physics*, *23*(2), 877–894. https://doi.org/10.5194/acp-23-877-2023

Fan, T., Liu, X., Ma, P.-L., Zhang, Q., Li, Z., Jiang, Y., et al. (2018). Emission or atmospheric processes? An attempt to attribute the source of large bias of aerosols in eastern China simulated by global climate models. *Atmospheric Chemistry and Physics*, *18*(2), 1395–1417. https://doi.org/10.5194/acp-18-1395-2018

Fankhauser, S., Smith, S. M., Allen, M., Axelsson, K., Hale, T., Hepburn, C., et al. (2022). The meaning of net zero and how to get it right. *Nature Climate Change*, *12*(1), 15–21. https://doi.org/10.1038/s41558-021-01245-w

Fischer, E. M., & Schär, C. (2009). Future changes in daily summer temperature variability: Driving processes and role for temperature extremes. *Climate Dynamics*, *33*(7), 917–935. https://doi.org/10.1007/s00382-008-0473-8

Fuhrer, J., Val Martin, M., Mills, G., Heald, C. L., Harmens, H., Hayes, F., et al. (2016). Current and future ozone risks to global terrestrial biodiversity and ecosystem processes. *Ecology and Evolution*, *6*(24), 8785–8799. https://doi.org/10.1002/ece3.2568

Gao, J., Yang, Y., Wang, H., Wang, P., Li, B., Li, J., et al. (2023). Climate responses in China to domestic and foreign aerosol changes due to clean air actions during 2013–2019. *Npj Climate and Atmospheric Science*, *6*, 1–10. https://doi.org/10.1038/s41612-023-00488-y

Gao, Y., Liao, H., Chen, H., Zhu, B., Hu, J., Ge, X., et al. (2022). Composite analysis of aerosol direct radiative effects on meteorology during wintertime severe haze events in the North China Plain. *Journal of Geophysical Research: Atmospheres*, *127*(18), e2022JD036902. https://doi.org/10.1029/2022JD036902

Gao, Z., Lenschow, D. H., He, Z., & Zhou, M. (2009). Seasonal and diurnal variations in moisture, heat and CO_2 fluxes over a typical steppe prairie in Inner Mongolia, China. *Hydrology and Earth System Sciences*, *13*(7), 987–998. https://doi.org/10.5194/hess-13-987-2009

Ge, J., Liu, Q., Zan, B., Lin, Z., Lu, S., Qiu, B., & Guo, W. (2022). Deforestation intensifies daily temperature variability in the northern extratropics. *Nature Communications*, *13*(1), 5955. https://doi.org/10.1038/s41467-022-33622-0

Guo, F., Do, V., Cooper, R., Huang, Y., Zhang, P., Ran, J., et al. (2021). Trends of temperature variability: Which variability and what health implications? *Science of the Total Environment*, *768*, 144487. https://doi.org/10.1016/j.scitotenv.2020.144487

Guo, Y., Barnett, A. G., Yu, W., Pan, X., Ye, X., Huang, C., & Tong, S. (2011). A large change in temperature between neighbouring days increases the risk of mortality. *PLoS One*, *6*(2), e16511. https://doi.org/10.1371/journal.pone.0016511

Hamal, K., & Pfahl, S. (2024). Physical processes leading to extreme day-to-day temperatures changes, part I: Present-day climate. *EGUsphere*, *2024*, 1–32. https://doi.org/10.5194/egusphere-2024-3732

Hansen, J., Sato, M., & Ruedy, R. (1997). Radiative forcing and climate response. *Journal of Geophysical Research*, *102*(D6), 6831–6864. https://doi.org/10.1029/96JD03436

He, J., Zhang, Y., Glotfelty, T., He, R., Bennartz, R., Rausch, J., & Sartelet, K. (2015). Decadal simulation and comprehensive evaluation of CESM/CAM 5.1 with advanced chemistry, aerosol microphysics, and aerosol-cloud interactions. *Journal of Advances in Modeling Earth Systems*, *7*(1), 110–141. https://doi.org/10.1002/2014MS000360

Hersbach, H., Bell, B., Berrisford, P., Biavati, G., Horányi, A., Muñoz Sabater, J., et al. (2023). ERA5 hourly data on single levels from 1940 to present. *Copernicus Climate Change Service (C3S) Climate Data Store (CDS)*. https://doi.org/10.24381/cds.adbb2d47

Horton, D. E., Johnson, N. C., Singh, D., Swain, D. L., Rajaratnam, B., & Diffenbaugh, N. S. (2015). Contribution of changes in atmospheric circulation patterns to extreme temperature trends. *Nature*, *522*(7557), 465–469. https://doi.org/10.1038/nature14550

Huang, M. T., & Zhai, P. M. (2021). Achieving Paris agreement temperature goals requires carbon neutrality by middle century with far-reaching transitions in the whole society. *Advances in Climate Change Research*, *12*(2), 281–286. https://doi.org/10.1016/j.accre.2021.03.004

Hurrell, J. W., Holland, M. M., Gent, P. R., Ghan, S., Kay, J. E., Kushner, P. J., et al. (2013). The community Earth system model: A framework for collaborative research. https://doi.org/10.1175/BAMS-D-12-00121.1

Irfan, M., Musarat, M. A., Alaloul, W. S., & Ghufran, M. (2024). Radiative forcing on climate change: Assessing the effect of greenhouse gases on energy balance of Earth. In *Advances and technology development in greenhouse gases: Emission, capture and conversion* (pp. 137–167). https://doi.org/10.1016/B978-0-443-19066-7.00012-6

Kamal, A. S. M. M., Hossain, F., & Shahid, S. (2021). Spatiotemporal changes in rainfall and droughts of Bangladesh for 1.5 and 2°C temperature rise scenarios of CMIP6 models. *Theoretical and Applied Climatology*, *146*(1), 527–542. https://doi.org/10.1007/s00704-021-03735-5

Katz, R. W., & Brown, B. G. (1992). Extreme events in a changing climate: Variability is more important than averages. *Climatic Change*, *21*(3), 289–302. https://doi.org/10.1007/bf00139728

Kim, D., Ray, R. L., & Choi, M. (2017). Simulations of energy balance components at snow-dominated montane watershed by land surface models. *Environmental Earth Sciences*, *76*(9), 1–17. https://doi.org/10.1007/s12665-017-6655-0

Kotz, M., Wenz, L., Stechemesser, A., Kalkuhl, M., & Levermann, A. (2021). Day-to-day temperature variability reduces economic growth. *Nature Climate Change*, *11*(4), 319–325. https://doi.org/10.1038/s41558-020-00985-5

Lei, Y., Wang, Z., Zhang, X., Che, H., Yue, X., Tian, C., et al. (2022). Avoided population exposure to extreme heat under two scenarios of global carbon neutrality by 2050 and 2060. *Environmental Research Letters*, *17*(9), 094041. https://doi.org/10.1088/1748-9326/ac8e1b

Li, M., Wang, T., Xie, M., Zhuang, B., Li, S., Han, Y., & Chen, P. (2017). Impacts of aerosol-radiation feedback on local air quality during a severe haze episode in Nanjing megacity, eastern China. *Tellus B: Chemical and Physical Meteorology*, *69*(1), 1339548. https://doi.org/10.1080/16000889.2017.1339548

Liao, H., Seinfeld, J. H., Adams, P. J., & Mickley, L. J. (2004). Global radiative forcing of coupled tropospheric ozone and aerosols in a unified general circulation model. *Journal of Geophysical Research*, *109*(D16), D16207. https://doi.org/10.1029/2003JD004456

Liu, Q. (2021). *A preliminary study on the climatological problems of interdiurnal temperature variability under global warming and their impacts on human health*. PhD Thesis. Nanjing University. Retrieved from https://oversea.cnki.net/index/

Liu, Q., Tan, Z. M., Sun, J., Hou, Y., Fu, C., & Wu, Z. (2020). Changing rapid weather variability increases influenza epidemic risk in a warming climate. *Environmental Research Letters*, *15*(4), 044004. https://doi.org/10.1088/1748-9326/ab70bc

Liu, X., Ma, P. L., Wang, H., Tilmes, S., Singh, B., Easter, R. C., et al. (2016). Description and evaluation of a new four-mode version of the modal aerosol module (MAM4) within version 5.3 of the community atmosphere model. *Geoscientific Model Development*, *9*(2), 505–522. https://doi.org/10.5194/gmd-9-505-2016

Piskala, V., & Huth, R. (2020). Asymmetry of day-to-day temperature changes and its causes. *Theoretical and Applied Climatology*, *140*(1–2), 683–690. https://doi.org/10.1007/s00704-020-03116-4

Ren, L., Yang, Y., Wang, H., Wang, P., Yue, X., & Liao, H. (2024). Co-benefits of mitigating aerosol pollution to future solar and wind energy in China toward carbon neutrality. *Geophysical Research Letters*, *51*(13), e2024GL109296. https://doi.org/10.1029/2024GL109296

Schär, C., Vidale, P. L., Lüthi, D., Frei, C., Häberli, C., Liniger, M. A., & Appenzeller, C. (2004). The role of increasing temperature variability in European summer heatwaves. *Nature*, *427*(6972), 332–336. https://doi.org/10.1038/nature02300

Schleussner, C. F., Rogelj, J., Schaeffer, M., Lissner, T., Licker, R., Fischer, E. M., et al. (2016). Science and policy characteristics of the Paris agreement temperature goal. *Nature Climate Change*, *6*(9), 827–835. https://doi.org/10.1038/nclimate3096

Soci, C., Hersbach, H., Simmons, A., Poli, P., Bell, B., Berrisford, P., et al. (2024). The ERA5 global reanalysis from 1940 to 2022. *Quarterly Journal of the Royal Meteorological Society*, *150*(764), 4014–4048. https://doi.org/10.1002/qj.4803

Tang, M., He, Y., Zhang, X., Li, H., Huang, C., Wang, C., et al. (2021). The acute effects of temperature variability on heart rate variability: A repeated-measure study. *Environmental Research*, *194*, 110655. https://doi.org/10.1016/j.envres.2020.110655

Van Wijngaarden, W. A., & Happer, W. (2020). Dependence of Earth's thermal radiation on five most abundant greenhouse gases. *arXiv preprint arXiv*, *2006*, 03098. https://doi.org/10.48550/arXiv.2006.03098

Wallace, J. M., & Hobbs, P. V. (2006). Atmospheric science: an introductory survey (Vol. 92).

Wang, F., Harindintwali, J. D., Yuan, Z., Wang, M., Wang, F., Li, S., et al. (2021). Technologies and perspectives for achieving carbon neutrality. *Innovation*, *2*(4), 100180. https://doi.org/10.1016/j.xinn.2021.100180

Wang, H., Easter, R. C., Rasch, P. J., Wang, M., Liu, X., Ghan, S. J., et al. (2013). Sensitivity of remote aerosol distributions to representation of cloud–aerosol interactions in a global climate model. *Geoscientific Model Development*, *6*(3), 765–782. https://doi.org/10.5194/gmd-6-765-2013

Wang, P. (2025). Data for "mitigated rapid temperature variability in the northern mid-high latitudes under carbon neutrality" [Dataset]. *Zenodo*. https://doi.org/10.5281/zenodo.15852907

Wang, P., Yang, Y., Xue, D., Ren, L., Tang, J., Leung, L. R., & Liao, H. (2023). Aerosols overtake greenhouse gases causing a warmer climate and more weather extremes toward carbon neutrality. *Nature Communications*, *14*(1), 7257. https://doi.org/10.1038/s41467-023-42891-2

Westervelt, D. M., Horowitz, L. W., Naik, V., Golaz, J. C., & Mauzerall, D. L. (2015). Radiative forcing and climate response to projected 21st century aerosol decreases. *Atmospheric Chemistry and Physics*, *15*(22), 12681–12703. https://doi.org/10.1038/s41612-023-00400-8

Wheeler, T. R., Craufurd, P. Q., Ellis, R. H., Porter, J. R., & Prasad, P. V. (2000). Temperature variability and the yield of annual crops. *Agriculture, Ecosystems & Environment*, *82*(1–3), 159–167. https://doi.org/10.1016/S0167-8809(00)00224-3

Wu, S., Luo, M., Lau, G. N. C., Zhang, W., Wang, L., Liu, Z., et al. (2025). Rapid flips between warm and cold extremes in a warming world. *Nature Communications*, *16*(1), 3543. https://doi.org/10.1038/s41467-025-58544-5

Xiang, B., Xie, S. P., Kang, S. M., & Kramer, R. J. (2023). An emerging Asian aerosol dipole pattern reshapes the Asian summer monsoon and exacerbates northern hemisphere warming. *Npj Climate and Atmospheric Science*, *6*(1), 77. https://doi.org/10.1038/s41612-023-00400-8

Xu, L., & Penner, J. E. (2012). Global simulations of nitrate and ammonium aerosols and their radiative effects. *Atmospheric Chemistry and Physics*, *12*(20), 9479–9504. https://doi.org/10.5194/acp-12-9479-2012

Yang, N., Xia, Y., Zhao, C., Xie, F., & Hu, S. (2024). Emission reductions during COVID-19 enhance marine heatwave over the North Pacific in spring 2020. *Climate Dynamics*, *62*(12), 10865–10880. https://doi.org/10.1007/s00382-024-07426-5

Yang, Y., Mou, S., Wang, H., Wang, P., Li, B., & Liao, H. (2024). Global source apportionment of aerosols into major emission regions and sectors over 1850–2017. *Atmospheric Chemistry and Physics*, *24*(11), 6509–6523. https://doi.org/10.5194/acp-24-6509-2024

Yao, N., Xi, H., Chen, L., Song, Z., Li, J., Chen, Y., et al. (2025). Effective climate policies for major emission reductions of ozone precursors: Global evidence from two decades. *arXiv preprint*, *2505*, 14731. https://doi.org/10.48550/arXiv.2505.14731

Zeng, L., Yang, Y., Wang, H., Wang, J., Li, J., Ren, L., et al. (2021). Intensified modulation of winter aerosol pollution in China by El Niño with short duration. *Atmospheric Chemistry and Physics*, *21*(13), 10745–10761. https://doi.org/10.5194/acp-21-10745-2021

Zhan, Z., Zhao, Y., Pang, S., Zhong, X., Wu, C., & Ding, Z. (2017). Temperature change between neighboring days and mortality in United States: A nationwide study. *Science of the Total Environment*, *584*, 1152–1161. https://doi.org/10.1016/j.scitotenv.2017.01.177

Zhang, B. (2020). The effect of aerosols to climate change and society. *Journal of Geoscience and Environment Protection*, *8*(8), 55–78. https://doi.org/10.4236/gep.2020.88006

Zhang, J., & You, Q. (2023). Avoidable heat risk under scenarios of carbon neutrality by mid-century. *Science of the Total Environment*, *892*, 164679. https://doi.org/10.1016/j.scitotenv.2023.164679

Zhu, J., Xie, A., Qin, X., & Xu, B. (2023). Assessment of future Antarctic amplification of surface temperature change under different Scenarios from CMIP6. *Journal of Mountain Science*, *20*, 1074–1089. https://doi.org/10.1007/s11629-022-7646-5